ICRF heating schemes for the ITER non-active phase

Mireille Schneider[1,*], *Jean-François* Artaud[2], *Paul* Bonoli[3], *Yevgen* Kazakov[4], *Philippe* Lamalle[1], *Ernesto* Lerche[4,5], *Dirk* Van Eester[4] and *John* Wright[3]

1 ITER Organization, Route de Vinon-sur-Verdon, CS 90 046, 13067 St. Paul-lez-Durance, France
2 CEA, IRFM, F-13108 Saint Paul-lez-Durance, France
3 Plasma Science and Fusion Center, MIT, Cambridge, MA 02139, USA
4 LPP-ERM/KMS, Association Eurofusion-Belgian State, TEC partner, Brussels, Belgium
5 Euratom/CCFE Fusion Association, Culham Science Centre, Abingdon, United Kingdom

Abstract. ITER plasma operation requires a non-active phase for tokamak initial commissioning, covering First Plasma and Pre-Fusion Power Operation phases, PFPO-1 and PFPO-2. Non-active operation consists of hydrogen and helium plasmas to minimize the neutron production rate. The present document describes some Ion Cyclotron Radio Frequency (ICRF) heating schemes in terms of their predicted performance for the main foreseen scenarios of the ITER non-active phase in hydrogen and helium. Emphasis is given on remaining issues and physics uncertainties to be addressed for successful ICRF heating in ITER.

1 Introduction

Auxiliary heating power is essential for future tokamaks to achieve and sustain fusion performance. In ITER, three auxiliary heating methods are foreseen: Electron Cyclotron Resonance Heating (ECRH), Ion Cyclotron Resonance Frequency heating (ICRF) and Neutral Beam Injection (NBI). The new ITER research plan is based on a staged approach including two Pre-Fusion Power Operation phases PFPO-1 and PFPO-2 consisting of hydrogen and helium plasmas. The ITER fusion operation phases, i.e. deuterium and deuterium-tritium plasmas, are not covered in the present analysis.

Efficient fusion performance relies on achieving an improved confinement regime, i.e. the so-called H-mode. The L-H power threshold is predicted by scaling laws derived from experimental database and mostly depends on the core density, the plasma surface area and the toroidal magnetic field [1].

Three main magnetic fields are now under consideration to improve H-mode access capabilities in the non-active phase: B_0 = 1.8T, 2.65T and 5.3T. The 5MA/1.8T operation is aimed at enabling H-mode access early in the plan, i.e. in the PFPO-1 phase where only ECRH and ICRF should be available (20 MW of ECRH and possibly 10 MW of ICRF if the PFPO-1 installation of one IC antenna is confirmed). The PFPO-2 phase will benefit from the full baseline heating capabilities, i.e. ECRH, ICRF and NBI heating providing a total auxiliary power of 73 MW. A number of ICRF heating schemes have been investigated for these magnetic fields, both in hydrogen and helium plasmas. The expected RF absorption efficiencies of each of these schemes, based on 1D RF wave modelling [2], is reported here.

* Corresponding author: mireille.schneider@iter.org

2 ICRF heating schemes

Transport simulations have been carried out using the METIS 0.5D transport code [3], which combines a 1D current diffusion solver, a 2D equilibrium solver and a hybrid 0D/1D calculation of heat transport dynamics, based on scaling laws. These simulations have provided a consistent initial set of temperatures and densities that are used for ICRF wave calculations [4], for which central core values are displayed in table 1 as a reference for scenarios covered in the present document.

Table 1. Central electron and ion temperatures and densities for all scenarios covered by this analysis.

B_0 (T)	**5.3**		**2.65**		**1.8**		**3**	**3.3**
I_p (MA)	15		7.5		5		8.5	9.5
P_{AUX} (MW)	30						73	
Main ion	H	He	H	He	H	He	H	H
Te^0 (keV)	10	13	7.2	11	14	16	14	11
Ti^0 (keV)	12	16	6.0	12	7.0	8.0	10	9.3
ne^0 (10^{19} m^{-3})	5.6	5.5	2.8	3.0	1.9	1.9	3.2	3.4
ni^0 (10^{19} m^{-3})	5.4	2.9	2.7	1.7	1.8	1.0	2.2	2.3

ICRF wave calculations have been performed with the TOMCAT 1D and TORIC 2D ICRF codes [2, 5]. In this analysis, only the core Single Pass Absorption (SPA), summed over electrons and ion species, is included, since it has been demonstrated to reliably quantify the quality of a heating scheme when compared to experiment, see e.g. [6]. All concentrations are given with respect to the electron density.

The ability of the antenna system to couple ICRF power to these plasmas through the edge region is not discussed in the present paper.

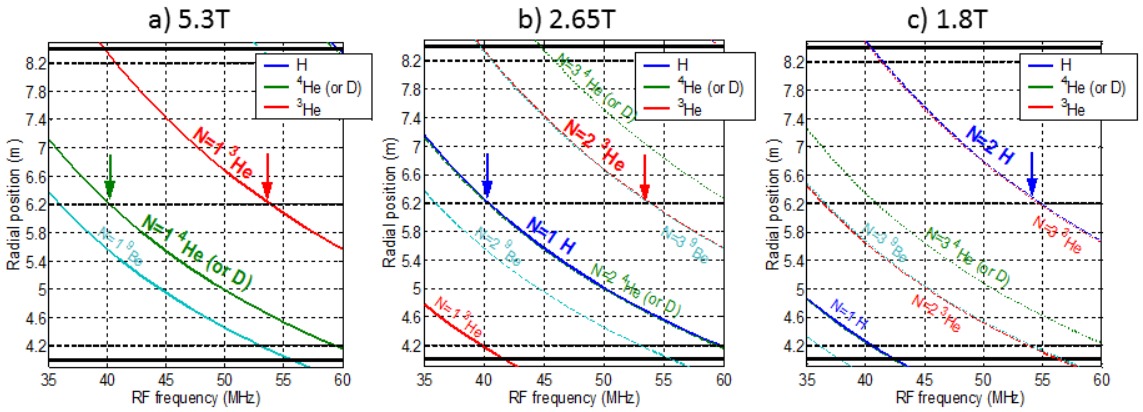

Fig. 1. Cyclotron resonance layers of H, He^4, He^3 and Be^9 ions as a function of the ICRF wave frequency at (a) 5.3T, (b) 2.65T and (c) 1.8T for left / middle / right figures respectively.

Various ion species have been taken into account to explore the best ICRF heating schemes in the ITER non-active phase: H, He^4, He^3 and Be^9. Majority ions can be heated at harmonics of the cyclotron resonance, while fundamental majority heating is inefficient due to the screening effect, i.e. when the wave electric field component rotating in the same sense as the ions vanishes at the resonance location of the majority ion [7]. Other ICRF heating schemes rely on the presence of a minority species with a charge-to-mass ratio different from the majority ion one. These are the two-ion minority heating schemes. Fundamental ion heating schemes typically work best at reduced concentration while harmonic heating requires preheating or a large ion population. H-He^4 mixtures have also been explored to investigate the three-ion minority heating schemes, based on the following fast wave property: if the L-cutoff layer of a two-ion plasma is located close to the fundamental cyclotron resonance of a third species, the latter, if present in small quantities, absorbs almost all the power [8]. Majority species, two-ion and three-ion heating schemes have been investigated at 5.3T, 2.65T and 1.8T, as described in the next paragraphs. Resonances of all considered ions are displayed in Figure 1 for the three values of the magnetic field as a function of the ICRF wave frequency, of which the accessible range in ITER is 40-55 MHz.

2.1 Heating schemes at a magnetic field of 5.3T

As illustrated in Figure 1.a, central heating can be achieved at 5.3T for fundamental resonance of He^3 at 53 MHz or fundamental resonance of He^4 at 40 MHz. Off-axis fundamental Be^9 heating is also possible at 40 MHz. Characteristics of associated heating schemes are summarized in Table 2 and subsequently discussed.

2.1.1 Hydrogen plasmas

Fundamental minority Be^9 heating exhibits a low absorption (SPA < 0.4) with dominant electron heating for a Be^9 level of 0.5%, which degrades at higher Be^9 concentration, leading to poor ICRF heating at full field.

Inverted schemes such as He^3 and He^4 heating in hydrogen are more appropriate. They are sensitive to the level of background impurity species, as observed at JET with a C-wall [9,10] and Be-wall [11,12]. Hence, the presence of Be^9 impurities in hydrogen influences the He^4 and He^3 cyclotron absorption in a similar way as D or He^4 dilution helps the He^3 absorption in the D or He^4-(He^3)-H three-ion scheme. An example is given in Figure 2, which shows that the higher the background Be^9 level, the lower the He^4 concentration can be, with equivalent absorption. There is no precise estimate of the Be^9 level in ITER, assumed to be ~2% in the core plasma transport modelling.

Table 2. Performance of various ICRF heating schemes at 15 MA / 5.3 T. Shaded cells highlight high SPA schemes.

Main ion	Heating scheme	f_{IC} (MHz)	SPA	Constraints and optimal conditions
H	n=1 min He^3 He^4-(He^3)-H	53	~ 0.95	$X[He^3]$ < 1% $X[He^4]$ ~ 10-15%
	n=1 min He^4 (He^4)-H and Be^9-(He^4)-H	41	0.6-0.8	$X[He^4]$ ~ 0.1-2% Depends on Be^9 level (see Figure 2)
	n=1 min He^3 (He^3)-H	53	~ 0.8 at $X[Be^9]$~1%	$X[He^3]$ ~ 2-4% Depends on Be^9 level
	n=1 min Be^9 (Be^9)-H	40	< 0.4 at $X[Be^9]$~0.5%	Low damping rate
He^4	n=1 min He^3 (He^3)-He^4	53	~ 0.8	$X[He^3]$ ~ 4-5%
	n=1 min Be^9 (Be^9)-He^4	40	< 0.25	Low damping rate
	n=1 maj He^4	40	~ 0.2	Low damping rate (E_+ screening)

The SPA for the (^{3}He)-H scheme is computed to maximize to ~ 0.8 for an He^3 concentration of ~ 2-4% assuming 1% of Be^9. Operating at lower He^3 concentrations would lead to a lower efficiency but may be desirable to limit the operation costs. As discussed above, the He^3 concentration can be reduced with equivalent efficiency if the Be^9 concentration is higher [10,12]. Similarly, heating He^4 as a minority in hydrogen is possible. While this regime was not accessible in JET-C wall operation [13] (Z/A ratio for C is the same as He^4 and D), changing the main intrinsic low-Z impurity from C to Be^9 allows this scheme to work. Indeed, since $(Z/A)_{Be9} < (Z/A)_{He4} < (Z/A)_H$, He^4 ions can be effectively heated at very low concentrations (~0.1-0.2%) via the Be^9-(He^4)-H scheme provided the core Be^9 concentration

* Corresponding author: mireille.schneider@iter.org

is ~2% (see Figure 2). If Be^9 level is low (<0.5%), then the absorption is maximized at higher $X[He^4]$ ~1%. Note that at $X[Be^9]$ > 3%, minority heating of He^4 ions becomes inefficient. Injecting Ne^{22} isotope (Z/A close to that for Be^9) could be an option to operate at very low He^4 levels, since controlling ^{9}Be is unlikely.

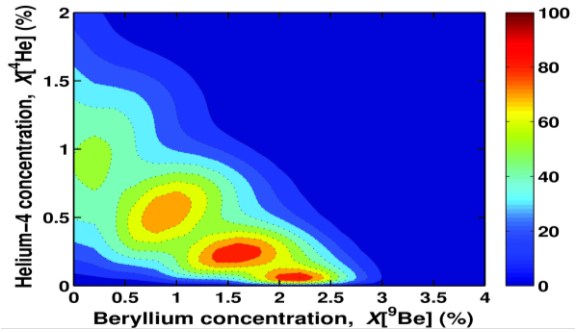

Fig. 2. Absorption by He^4 in H wrt $X[Be^9]$ and $X[He^4]$.

The three-ion heating scheme offers a more interesting option as its efficiency relies on very low minority concentration: heating He^3 ions with $X[He^3]$ < 1% in H-He^4 plasmas ($X[He^4]$ ~ 10-15%) provides a SPA of 0.95 making it the best absorption scheme, as experimentally demonstrated at JET and C-mod [14].

However, controlling the He^3 concentration in the presence of He^4 is challenging, since spectroscopy measurement can generally not distinguish them. They may however be discriminated by their different widths in wavelengths since He^3 ions are ICRF-accelerated while He^4 ions remain thermal [15]. An alternative is to inject a prepared He^4:He^3 mixture in the machine.

2.1.2 Helium plasmas

Fundamental majority He^4 heating exhibits a low absorption (SPA ~ 0.24) due to the E_+ screening effect, as discussed above. The situation may improve at higher temperatures due to enhanced Doppler-broadening, taking the vanishing E_+ point away from the resonance, as observed in JET-C in NBI preheated plasmas [16].

Fundamental minority Be^9 heating presents a SPA < 0.25 with dominant electron heating. Hence, the best heating scheme in helium at 5.3T is fundamental minority He^3 with a SPA of 0.8. It however requires He^3 concentration ~ 4-5 % which is scarce and costly.

2.2 Heating schemes at a magnetic field of 2.65T

Figure 1.b indicates that, at 2.65T, central deposition can be achieved with fundamental H or second harmonic He^4 heating at 40 MHz, and with second harmonic He^3 heating at 53 MHz. Characteristics and performance of investigated heating schemes are summarized in Table 3.

2.2.1 Hydrogen plasmas

Fundamental majority H heating exhibits a low absorption (SPA ~ 0.22) due to the screening effect. Again, the screening could be reduced by the Doppler-broadening at higher temperature but it has not been investigated yet. Second harmonic minority He^3 heating provides no significant improvement with a SPA < 0.25, even at high He^3 concentration. Both schemes have been tested in JET-C and the poor heating performance was confirmed [6]. Finally, second harmonic minority He^4 heating is a better heating scheme, providing a SPA still below 0.5 and with a dominant electron heating, leading to a very broad deposition. Thus, there is no efficient ICRF scheme at 2.65T in hydrogen. For this reason, optional schemes are envisaged at 3T / 3.3T to provide an operational space close to half field with an efficient ICRF heating scheme, as described in section 2.4.

Table 3. Performance of various ICRF heating schemes at 7.5 MA / 2.65T. Shaded cells highlight high SPA schemes.

Main ion	Heating scheme	f_{IC} (MHz)	SPA	Constraints and optimal conditions
H	n=2 min He^4	40	< 0.5	Even at high X[He^4]; dominant on electrons
	n=2 min He^3	53	< 0.25	Even at high X[He^3]
	n=1 maj H	40	~ 0.22	Low damping rate (E_+ screening)
He^4	n=1 min H	40	~ 1	X[H] ~ 2-8%
	n=2 maj He^4	40	0.78	-
	n=2 min He^3	53	> 0.6	X[He^3]>5%, off-axis He^4 absorption

2.2.2 Helium plasmas

Second harmonic minority He^3 heating displays a SPA of 0.6 with rather high concentration of He^3, here above 5%, hence this scheme should not be favoured. Second harmonic majority He^4 heating shows a SPA of 0.78, making it a suitable candidate. Finally, fundamental minority H heating at 40 MHz is the best candidate with a SPA close to 1 and X[H]~2-8%. The scheme could probably still be efficient at higher H concentration, which may not be avoidable due to the dilution effect when injecting hydrogen pellets into helium plasmas.

2.3 Heating schemes at a magnetic field of 1.8T

Operating at low magnetic field of 1.8T may enable H-mode operation during the PFPO-1 phase where auxiliary heating will be provided by 20 MW of ECRH and probably 10 MW of ICRF (one IC antenna may be installed for this phase but it is still under evaluation). Operating at low density is essential to minimize the L-H power threshold. 40% of the Greenwald density is considered as optimal as described in [17]. The threshold rollover at lower density can be due to the strong electron-ion decoupling, leading to $T_e \gg T_i$, where TEM and ETG modes may play a role and METIS scaling laws are beyond their validity domain. Hence, kinetic profiles used for this modelling need comparison with other transport codes. Operating at such low magnetic field induces an overcompensation of the magnetic field ripple by ferromagnetic inserts, leading to a ripple of the order of -1.3% which could enhance fast ion losses, still to be quantified. In addition, low density means low collisionality, further reducing the fast ion confinement, potentially leading to enhanced RF-induced plasma wall interaction [18].

As illustrated in Figure 1.c, central resonances are available at 1.8T for third harmonic He^4 at 40 MHz, and

second harmonic H or third harmonic He^3 at 55 MHz. All these schemes are summarized in Table 4.

Table 4. Performance of various ICRF heating schemes at 5 MA / 1.8T. Shaded cells highlight high SPA schemes.

Main ion	Heating scheme	f_{IC} (MHz)	SPA	Constraints and optimal conditions
H	n=2 maj H	53	~ 1	-
	n=3 min He^4	40	~ 0.5	Even at high X[He^4]; dominant on electrons
He^4	n=2 min H	53	~ 1	X[H] = 5%
	n=3 maj He^4	40	~ 0.77	Dominant el
	n=3 min He^3	53	> 0.7	Even at high X[He^3]; dominant on electrons

2.3.1 Hydrogen plasmas

Third harmonic minority He^4 heating exhibits a SPA of 0.5 with dominant electron heating, even at high He^4 concentration. The best scheme is second harmonic majority H heating with a very good SPA close to 1, making it an excellent scheme, provided the fast ions generated by harmonic heating are properly confined.

2.3.2 Helium plasmas

Third harmonic minority He^3 heating shows a SPA ~ 0.7 with dominant electron heating (> 0.8), even at high He^3 concentration: in this case and more generally when there is no adequate ion resonance, one can rely on Fast Wave Electron Heating and avoid He^3 injection. This generates broader deposition profiles but with an overall good absorption. Third harmonic majority He^4 heating shows a SPA of 0.77, again with dominant electron heating. Finally, second harmonic minority H heating shows a SPA close to 1, making it the best candidate. Good minority heating at cyclotron harmonics is unusual but can be achieved thanks to the beneficial $1/B_0^2$ scaling of the Finite Larmor Radius absorption [19].

2.4 Optional schemes at 3T & 3.3T in hydrogen

To compensate the lack of efficient ICRF scheme in hydrogen at 2.65T, one option is to increase the magnetic field to 3T or 3.3T and heat a small amount of He^3 (~1%) at its fundamental resonance at 40 MHz. Minimizing the He^3 level to ~0.05% can be achieved in a H-He^4 mixture with ~10-15% of He^4 ions (three-ion scheme). Under these conditions, the SPA is ~0.8-0.9 shared between central electron heating and off-axis He^3 ion heating on the HFS as illustrated in Figure 3.

These optional heating schemes could offer the possibility to reach H-mode in hydrogen when operating close to half field, enabling long pulse operation and ELM control at q_{95}=3. Adding 10-15% of He^4 reduces the minimum allowable operational density with respect to NBI shinethrough, and could allow access to hydrogenic H-mode operation at lower input power, if observations from recent JET experiments are confirmed [20]. However, tungsten accumulation with reduced central heating needs to be considered and quantified. Furthermore, as discussed above, He^3 level control in the presence of He^4 may prove challenging. Finally, ion losses are still to be assessed. They can be significant due to off-axis fast trapped ion acceleration [21]. They can however always be reduced by increasing the He^3 concentration to reduce the fast ion tail.

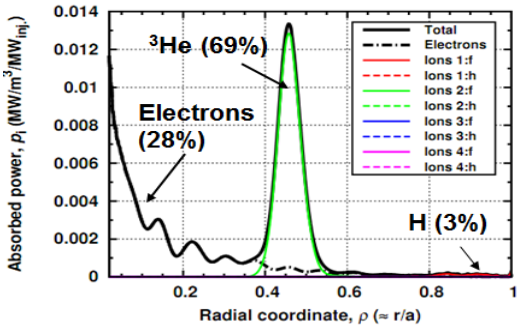

Fig. 3. Wave absorption for fundamental minority He^3 heating in an H:He^4 mixture at 3.3T (TORIC run).

3 Conclusion

Various ICRF heating schemes for the ITER non-active phase have been investigated. For the ITER ICRF frequency range 40-55 MHz, effective absorption schemes are available in hydrogen and helium at magnetic fields of 5.3T, 2.65T and 1.8T, except for hydrogen operation at 2.65T. This may be compensated by optional schemes at 3T and 3.3T with fundamental minority He^3 heating in a H-He^4 mixture (three-ion heating scheme). Results at 5MA/1.8T are preliminary as they imply a regime with strong electron / ion decoupling ($T_e >> T_i$) where TEM and ETG modes play a significant role, not covered by METIS scaling laws. Hence, kinetic profiles need to be crosschecked with other transport codes and made self-consistent with heating sources. Furthermore, most of the results presented in this paper have been produced by the TOMCAT 1D code and should be advanced with 2D full wave computations. Future antenna coupling studies will also contribute to complete the picture.

Acknowledgments

ITER is a Nuclear Facility INB-174. The views and opinions expressed herein do not necessarily reflect those of the ITER Organization.

References

1. Y.R. Martin et al, J. of Physics: Conf. Series **123** (2008) 012033
2. D. Van Eester and R. Koch, PPCF **40**, 1949–1975 (1998)
3. J.F. Artaud et al 2010 Nucl. Fusion **50** 043001
4. M. Schneider, 17th ITPA-IOS TG meeting – Naka, Japan (2016)
5. M. Brambilla, PPCF **41**, 1–34 (1999).
6. E. Lerche et al, PPCF 54 (2012) 069601 (6pp)
7. T. Stix, Waves in Plasmas, AIP Press (1992)
8. Ye.O. Kazakov et al, Nucl Fusion **55**, 032001 (2015)
9. M.-L. Mayoral et al, Nucl. Fusion 46 (2006) S550–S563
10. D. Van Eester et al, PPCF 51 (2009) 044007
11. D. Van Eester et al, EPS 2015 Lisbon (Portugal), P2.117
12. D. Van Eester et al, this conference
13. P. Lamalle et al. Nucl. Fusion 46, 391-400 (2006)
14. Ye.O. Kazakov et al., APS. 61, APS-DPP 2016, San Jose (USA)
15. M. von Hellerman et al., ITPA-EP, Seville (Spain), April 2017.
16. A. Krasilnikov et al, A V Krasilnikov et al 2009 PPCF 51 044005
17. F. Ryter et al, Nucl. Fusion **54** 083003 (2014)
18. E. Lerche et al, AIP Conference proceedings, 1689 (2015) 040003
19. M. Porkolab AIP Conference Proceedings 314, 99 (1994)
20. J. Hillesheim et al.,26th IAEA FEC, Kyoto, Japan, 2016., EX/5-2
21. J. Joly et al, this conference.